Epithelium-Innate Immune Cell Axis in Mucosal Responses to SIV

L. Shang[1], **L. Duan**[1], **K. E. Perkey**[1], **S. Wietgrefe**[1], **M. Zupancic**[1], **A. J. Smith**[1], **P. J. Southern**[1,*], **R. P. Johnson**[2], and **A. T. Haase**[1]

[1]Department of Microbiology and Immunology, Medical School, University of Minnesota, Minneapolis, MN 55455

[2]Yerkes National Primate Research Center, Emory University, Atlanta, GA 30322

Abstract

In the SIV-rhesus macaque model of HIV-1 transmission to women, one hallmark of the mucosal response to exposure to high doses of SIV is CD4 T cell recruitment that fuels local virus expansion in early infection. In this study, we systematically analyzed the cellular events and chemoattractant profiles in cervical tissues that precede CD4 T cell recruitment. We show that vaginal exposure to the SIV inoculum rapidly induces chemokine expression in cervical epithelium including CCL3, CCL20, and CXCL8. The chemokine expression is associated with early recruitment of macrophages and plasmacytoid dendritic cells that are co-clustered underneath the cervical epithelium. Production of chemokines CCL3 and CXCL8 by these cells in turn generates a chemokine gradient that is spatially correlated with the recruitment of CD4 T cells. We further show that the protection of SIVmac239 nef vaccination against vaginal challenge is correlated with the absence of this epithelium-innate immune cell-CD4 T cell axis response in the cervical mucosa. Our results reveal a critical role for cervical epithelium in initiating early mucosal responses to vaginal infection, highlight an important role for macrophages in target cell recruitment and provide further evidence of a paradoxical dampening effect of a protective vaccine on these early mucosal responses.

Keywords

SIV; Female Genital Tract; Mucosa; Cervix; Epithelium; Macrophage; pDC; CD4 T cell; Chemokine; Focal Cluster; Early Events; Cell Recruitment; SIV nef; Epithelium-Innate Immune Cell Axis

Introduction

Antiretroviral therapy has greatly reduced the morbidity and mortality from HIV-1 (Human Immunodeficiency Virus Type I) infection, and there has been continued progress as well in

Correspondence to: Ashley T. Haase, Department of Microbiology and Immunology, Medical School, University of Minnesota, 689 23rd Avenue S.E., Minneapolis, MN 55455-1507. Phone: 612-624-4442. Fax: 612-626-0623. haase001@umn.edu.
*Current address: Bridge-to-MD Program, One Battery Park Plaza, New York, NY 10004.

strategies and methods to prevent HIV transmission, e.g., the ALVAC-AIDSVAX vaccine,[1] topical and systemic pre-exposure prophylaxis,[2–6] treatment as prevention,[7] and male circumcision.[8–11] Nonetheless, even more effective prevention strategies are required to ultimately end the HIV/AIDS pandemic.

To that end, we have been seeking novel concepts and strategies for prevention through a deeper understanding of HIV-1 infection and transmission at mucosal surfaces, where the great majority of new HIV-1 infections are acquired.[12] We have specifically focused on the very early events in cervical vaginal mucosa in the studies carried out in the SIV (Simian Immunodeficiency Virus)-rhesus macaque model of HIV-1 sexual transmission to women.[13,14] In this non-human primate animal model, we have shown that small founder populations of infected cells are established and expand in the cervicovaginal mucosa prior to systemic dissemination and infection in a time frame equivalent to the eclipse phase of HIV-1 transmission ~10 days after exposure.[15] We have also shown that cervical epithelium plays an important role in facilitating local expansion of the founder populations of infected cells that precedes virus dissemination and a robust systemic infection.

We initially discovered that vaginal inoculation of high doses of SIV elicited increased expression of MIP-3α/CCL20 in cervical epithelium,[16,17] which was associated with recruitment of CCR6^{+} plasmacytoid dendritic cells (pDC) beneath the epithelium. The pDCs in turn produced the beta-chemokines, MIP-1α/CCL3 and MIP-1β/CCL4, to recruit CD4 T cells to fuel local virus expansion.[16,17] More recently, in studies of the NK cell response in the female reproductive tract (FRT) to vaginal inoculation of SIV,[18] we were struck by the extent of macrophage recruitment at 7 days after inoculation (7 d.p.i.) in addition to the previously reported recruitment of pDCs.[17] We therefore undertook a larger systematic investigation of the innate immune cells and chemokine signaling that precede and mediate CD4 T cell recruitment into the FRT. We report further evidence that the cervical epithelium initiates the response to vaginal inoculation of SIV, but also now show that focal accumulations of pDCs and macrophages themselves comprise an environment for concentrating chemokines and their receptors to efficiently recruit CD4 T cells at sites of infection. Remarkably, SIV nef vaccination disrupts this circuitry, thus serving as an example of novel strategies for prevention aimed at the mucosal epithelial-immune system axis to block the transmission-facilitating recruitment of CD4 T cells.

Results

In the studies reported here, we focused on the potential relationships between epithelial signaling and innate immune responses that could recruit CD4 T cells into the transition zone of the ectocervix and endocervix and adjoining endocervix, because this is the site where small founder populations of infected cells (viral (v)RNA+) have been most consistently detected, and the site where the influx of CD4 T cell targets has been associated with the local expansion of infection at 7 d.p.i. (co-clustering of CD4 T cells and vRNA+ CD4 T cells is illustrated in Figure 1 and described in references 13, 14, 16 and 17. It is also a site where increasing evidence supports an active role of the epithelium in orchestrating the response to SIV.[19] Thus this endocervical region is a promising site to extend our understanding of the relationships between the cervical epithelium and innate immune

responses to SIV. We also used a high dose of virus in order to increase the likelihood of sampling key events in FRT tissues.

Kinetics of cell recruitment and co-localization of vRNA⁺ cells, CD4 T cells, pDCs, and macrophages beneath cervical epithelium

Following high dose vaginal inoculation, local expansion of small founder populations of infected cells is driven by the influx of CD4 T cells in the cervical transition zone.[14,17] Here we show a detailed kinetics of CD4 T cell recruitment in cervical tissues (Fig. 2A). Consistent with previous observations,[14,17] cervical CD4 T cells are rare in uninfected animals, but their numbers were significantly increased by 7 d.p.i. (Fig. 2A). The massive CD4 influx into cervical tissues peaked at 14 d.p.i., and then declined, but to levels still considerably higher than baseline levels by 28 d.p.i., the last time point at which archived tissues were obtained in these studies of acute SIV infection following vaginal inoculation.[14] We found that the recruited CD4 T cells were clustered into foci in close proximity to the larger number of epithelial cells in the palmate folds of the endocervix near the transition zone at 7 d.p.i. (Fig. 2B). Further examination of earlier tissues demonstrated that even though the increase in CD4 T cells in cervical tissue by 4–6 d.p.i. did not reach statistical significance at the population level, in 3 out of 7 animals, accumulation of recruited CD4 T cells in local foci was already evident as early as 3 d.p.i. (Fig. 2B). By 7 d.p.i., local expansion in vRNA+ cells predominantly mapped to these foci (Fig. 2C) where the infected cells co-cluster with CD4 T cells.[14, 17] One such cluster is encircled and enlarged in Figure 1. The majority of vRNA+ cells were CD4 T cells; fewer than 5% vRNA+ cells were macrophages, as we had shown previously.[14,17,20] We later discuss the small proportion of infected macrophages despite their high frequency in these foci.

In addition to increased numbers of CD4 T cells underlying cervical epithelium, we also observed increases in numbers of macrophages (CD68⁺ and CD163⁺) and pDCs (CD123⁺ and BDCA-2⁺) (Fig. 3). The number of sub-epithelial macrophages increased rapidly within 1–3 d.p.i. and peaked at 4–6 d.p.i., followed by a decline to levels of about twice higher than baseline levels (Fig. 3A–B). Similarly, the number of sub-epithelial pDCs also increased significantly by 3 d.p.i., peaked at 7 d.p.i., and then remained at the higher levels through 14 d.p.i. (Fig. 3C–D).

There was thus both temporal and spatial evidence consistent with the hypothesis that macrophages as well as pDCs could play an important role in recruiting CD4 T cells into cervical foci to facilitate local expansion of infection. First, the kinetic analysis showed that both macrophages and pDCs were recruited into the cervical tissues slightly before CD4 T cells, and were thus temporally antecedent to CD4 T cell recruitment (Fig. 2A and Fig. 3). Second, macrophages and pDCs often accumulated in clusters beneath the epithelium lining the endocervix (Fig. 4A–B), consistently observed prior to CD4 T cell recruitment (Fig. 4). By 7 d.p.i., these clusters were comprised of CD4 T cells co-localizing with vRNA⁺ cells (Fig. 4C–F) and subepithelial pDCs and macrophages (immune cells were only rarely found in between epithelial cells) (Fig. 4G–H).

We also determined the temporal and spatial profiles of recruitment of other types of leukocytes in the cervical tissues besides CD4 T cells, macrophages, and pDCs at the same

time points (Table 1). First, eosinophils, basophils, plasma cells, and myeloid dendritic cells were absent in all examined cervical tissues before and after vaginal infection. Second, B cells, neutrophils, and CD8 T cells were only occasionally detected in cervical tissues close to the transition zone regardless of the status of infection, and were not co-localized with CD4 T cell foci. Third, consistent with previous reports, Langerhans cells were only located in the ectocervical epithelium,[21] thereby spatially separated from the CD4 T cell foci. Fourth, that even though a small number of NK cells infiltrated cervical tissues after vaginal infection, they were also spatially separated from CD4 T cell foci and vRNA+ cells.[18] Finally, we observed a slight increase in mast cells in the cervical tissues at 7 d.p.i. (Fig. 5). However, the spatial distribution of mast cells showed no evidence of co-clustering with CD4 T cells and vRNA+ cells (data not shown). Based on these results, we conclude that other cell types of leukocytes do not show a consistent and commensurate increase in size of the population as a potential source of chemokines that precedes CD4 T cell recruitment, nor do they co-localize with local CD4 T cell clusters and vRNA+ cells. Thus, they were not quantitatively, temporally, or spatially associated with CD4 T cell recruitment and local expansion of infection.

Cervical epithelium-innate immune cell axis and CD4 T cell recruitment

Based on the spatiotemporal profiles of macrophage, pDC, and CD4 T cell accumulation in cervical tissues, we hypothesized the following mechanism for CD4 T cell recruitment: cervical epithelium produces chemokines after vaginal inoculation to initiate the recruitment of macrophages and pDCs beneath the epithelium; the recruited macrophages and pDCs accumulate in clusters to serve as a concentrated source of chemokines, and this chemokine gradient drives the initial recruitment of CD4 T cells into these clusters. This mechanism extends the previous model of cell recruitment, in which pDCs were recruited as a source of beta-chemokines by epithelium-expressed CCL20,[17] by attributing an important new role for macrophages in this process. In addition, this mechanism enlarges our view of hypothesized mechanisms for CD4 T cell recruitment, where macrophages and pDCs in clusters become a source of chemokine ligands that produce a gradient to recruit more macrophages, pDCs, and CD4 T cells.

We tested predictions of this feed-forward mechanism by determining the profiles of chemokine expression in the epithelium and macrophages. We first confirmed the expression of CCL20 in the epithelium (Fig. 6A), and newly found that CCL3 and CXCL8 expression rapidly increased in epithelium compared to uninfected animals not exposed vaginally to SIV, both at the level of mRNA from microarray analysis (Fig. 6B), and at the protein level by immunohistochemical staining and quantitative image analysis (Fig. 6C). Expression of CCL3, CCL20, and CXCL8 on the cervical epithelium increased by 1 d.p.i., and thereafter remained elevated in naive animals, but, remarkably, in the vaccinated animals expression did not increase following vaginal exposure (Fig. 6A–C), an observation we discuss below.

This profile of chemokine ligand expression is consistent with the observed early recruitment of CCR5+ CCR6+, CXCR1+, and CXCR2+ macrophages (Fig. 7A); CCR6+, CXCR1+, and CXCR3+ pDCs (Fig. 7B); and subsequent recruitment of CCR5+, CCR6+, CXCR1+, and CXCR2+ CD4 T cells (Fig. 7C). Note that the macrophages in these foci were

also CCL3^{+}, CCL5^{+}, and CXCL8^{+} (Fig. 7A); and the pDCs were CCL5^{+} as well as CCL3^{+} and CCL4^{+}, as previously reported[17] (Fig. 7B). Moreover, the macrophages, but not the pDCs in these foci, were CXCL10^{+}, consistent with a primary role of macrophages in recruiting CXCR3^{+} pDCs and CD4 T cells (Fig. 7). We further discovered in this chemokine profiling that the recruited CD4 T cells themselves produced β-chemokines (Fig. 7C). Thus, the cells in these foci concentrate chemokines beneath the cervical epithelium close to the transformation zone (Fig. 8) that by a positive feed-forward loop mechanism maximize the availability of CD4 T cell targets in spatial proximity to infected cells to fuel expansion of the infected founder population in the endocervix.

Quiescent cervical epithelium-innate immune cell axis as a correlation of protection in SIV nef-vaccinated animals

In our hypothesized model, early activation of the cervical epithelium plays a critical role in initiating the cascade of innate cell infiltration leading to CD4 T cell recruitment in naive animals. By contrast, SIVmac239 nef vaccination[22,23,24] has recently been shown to inhibit the recruitment of CD4 T cells and subsequent local expansion of infected cells in the FRT mucosa, as one correlate of the protection against high dose vaginal challenge.[19,25] Because the numbers of cervical macrophages and pDCs in vaccinated animals also remained at the same levels as naive animals after challenge,[18,25] we examined the potential role of epithelial responses in the cervix of vaccinated animals in the inhibition of cell recruitment. In striking contrast to unvaccinated animals, expression of CCL3, CCL20, and CXCL8 by the cervical epithelium was not detected even 7 days after high dose vaginal challenge (Fig. 6A–C). These results imply that the protection mediated by SIVmac239 nef vaccine is correlated in part with the absence of an early activation signaling triggered in the cervical epithelium, and the subsequent recruitment of CD4 T cells.

Discussion

We have previously[14,17] shown that: 1) vaginal exposure to high doses of SIV infection elicited MIP-3α/CCL20 expression in the endocervical epithelium; 2) MIP-3α/CCL20 expression was subsequently associated with recruitment of β-chemokine-producing pDCs (CCR6^{+}); and 3) subsequent recruitment of CD4 T cell targets to fuel the local expansion of infection in the cervical tissues. In this study, we systematically analyzed the locations, quantities, and kinetics of accumulation of different types of leukocytes in cervical tissues after vaginal inoculation. Focusing on early mucosal events, we examined the spatial and temporal profiles of the expression of chemokines and chemokine receptors in the cervix. The two principal findings from this work are: (1) new evidence for the role of the cervical epithelium in initiating CD4 T cell recruitment; and (2) a new amplification mechanism mediated by focally clustered macrophages and pDCs to sustain CD4 T cell recruitment.

Here we provide evidence for the following sequential events in CD4 T cell recruitment (Fig. 9): 1) cervical epithelium responds to inoculation by producing CCL3, CCL20, and CXCL8; 2) the epithelial chemokines are spatiotemporally associated with and contribute to the recruitment of macrophages and pDCs, which co-cluster beneath the epithelium; 3) the macrophages and pDCs themselves produce CCL3, CCL5, CXCL8, and CXCL10 to create a

focal concentrated source of chemokines beneath the epithelium; 4) this chemokine concentration gradient is spatiotemporally associated with the recruitment of β-chemokine-producing CD4 T cells along with more macrophages and pDCs to generate a positive feed forward mechanism to sustain further increases in CD4 T cell targets.

Bringing CD4 T cells, macrophages, and pDCs together in close proximity beneath cervical epithelium provides a mechanism to account for the association and likelihood of finding most of the vRNA^{+} cells in these clusters. Note that since pDCs are the major producer of IFN-α in the cervical tissues as shown previously,[17] the clusters may provide a site of high levels of interferon to select for transmitted founder viruses with relatively greater IFN-α resistance.[26] Thus, clustering of recruited innate immune cells and CD4 T cells underneath the cervical epithelium represents a key early event to facilitate mucosal transmission.

While this reconstruction of early mucosal events gives an explanation of the co-clustering of mainly vRNA[+] CD4 T cells that lack markers of activation,[17] it raises the interesting question of why no more than about 5 percent of the vRNA^{+} cells are macrophages[17,27] even though they are CD4^{+}CCR5^{+}. Perhaps macrophage-specific restriction factors e.g. SAMHD1,[28,29] the activation state of the macrophages, or responsiveness to of IFN-α produced by pDCs make the macrophages less permissive to productive infection.

This study further extends the concept of a spatiotemporal signaling axis from epithelium to innate immune cells, and then to CD4 T cell targets to support local expansion of infection. The high dose challenge model used in order to increase the likelihood of sampling key events in FRT tissues most resembles the highest rates of HIV transmission seen in the acute stage of infection, where viral loads (VL) can exceed 10^5 copies of HIV-1 RNA/mL. Nonetheless, elements of this model are likely relevant to HIV heterosexual transmission to women exposed to lower doses of virus. First, unprotected sexual intercourse and exposure to seminal components increase macrophages and CD4 T target cells in human cervical tissues[30] via processes possibly initiated by the genital epithelium. Second, local immune activation contributes to the high risk of HIV acquisition in African women, probably due to the local production of CD4 T cell-recruiting chemokines.[31, 32] In addition, a low level of CD4 T cell-recruiting chemokines in the cervicovaginal compartment is associated with highly HIV-1-exposed seronegative (HESN) individuals.[33]

Thus interventions based on interrupting this signaling axis may guide potential strategies for preventing HIV transmission to women. We previously showed that one correlate of the maturation of protection by SIVmac239 nef vaccination is the formation of immune complexes that interact with the inhibitory receptor FcγR2b in the epithelium, which then generates factors that inhibit downstream events associated with a pro-inflammatory response and CD4 T cell recruitment.[19] Here we show direct effects associated with SIVmac239 nef vaccination on inhibiting chemokine expression in the epithelium. This is consistent with the concept that the multiple overlapping and complementary pathways involved in the epithelial response to SIV can be targeted by prevention strategies such as vaccination and the microbicide, glycerol monolaurate, which is thought to protect by interfering with the epithelial outside-in signaling.[17] Further exploration of approaches to

disrupt these signaling pathways thus could provide additional novel strategies for prevention.

Methods

Tissues from SIV-infected animals

New tissue sections were cut for the studies described here from archived genital tissues from previous studies of SIV high-dose vaginal infection[14,20] and SIVmac239 nef vaccine.[22] Briefly, in those studies, monkeys had been inoculated intravaginally with pathogenic SIVmac251 twice in a single day, with a 4-hour interval between inoculations. Each inoculation contained 1ml virus stock of 10^5 TCID50. Fresh tissues obtained at necropsy were fixed in 4% paraformaldehyde or SAFEFIX II (Fisher Scientific, Kalamazoo MI), and embedded in paraffin as previously reported.[14] In the cohort of SIV high dose vaginal infection, necropsy was carried out at day 0, 1, 3, 4, 5, 6, 7, 14, and 28 post infection (d.p.i.). In the SIV nef vaccine study, necropsy was carried out at day 0, 4, 5, 7, 11, and 14 post challenge (d.p.c.) in vaccinated animals.

Immunohistochemistry (IHC)

Single and double immunohistochemical staining (IHC), fluorescent immunohistochemical staining (IHC), and quantitative image analysis (QIA) were performed as described elsewhere.[34,35] The primary Abs used in this study are summarized in Table 2. In brief, tissue sections were deparaffinized in xylene and rehydrated in PBS. After blocking in Background Sniper (Biocare Medical, Concord CA), sections were incubated with primary Abs at 4°C overnight. Then signals were amplified with either 2° Ab-Biotin + ABC Kit (Vector Lab, Burlingame CA) in IHC or Alexa Fluor dyes (Invitrogen, Eugene OR) in FIHC. Nuclei were counterstained with hematoxylin or TOTO-3 (Invitrogen, Eugene OR) respectively. Images and montages were taken on Olympus BX60 and Olympus Fluoview FV1000 (Olympus, USA). To measure the kinetics of leukocyte accumulation, we manually counted cells in the entire cervical transition zones of all examined sections. The tissue areas and pixels/intensities were measured by the Aperio Scanscope System (Leica, Buffalo Grove IL).

Toluidine staining of mast cells

Tissue sections were deparaffinized in xylene, rehydrated in water, and stained in toluidine blue solution for 2–3 minutes. Then the slides were thoroughly washed in distill water, quickly dehydrated in 100% ethanol, and cleared in xylene. The toluidine blue solution contains freshly mixed 1% toluidine blue O/70% ethanol and 1% $NaCl/H_2O$ pH2.3 (1:9 v:v) (Sigma-Aldrich, St Louis MO).

In situ hybridization (ISH)

SIV RNA was detected in paraformaldehyde-fixed and paraffin-embedded tissues by in situ hybridization as previously described.[14] Briefly, sections were deparaffinized in xylene, rehydrated in PBS, and permeablized sequentially in HCl, digitonin, and proteinase K. The sections were then acetylated and hybridized to ^{35}S-labeled SIV-specific riboprobes. After washing and digestion with ribonucleases, the sections were coated with nuclear-track

emulsion before exposure and development. For fluorescent ISH, digoxigenin-labeled SIV-specific riboprobes were used, and followed by sequential staining with Goat anti-digoxigenin Abs (Roche, Indianapolis, IN) and Donkey anti-Goat Abs conjugated with Alexa Fluor 555 (Invitrogen, Eugene, OR).[34,35]

Statistical tests

The Wilcoxon rank-sum test was used to measure the variations in leukocytes over the course of infection. Statistical analyses were carried out using Prism 4 software.

Supplementary Material

Refer to Web version on PubMed Central for supplementary material.

Acknowledgments

Abbreviations used in this article

| **d.p.c.** | day post challenge |
d.p.i.	day post infection
FRT	female reproductive tract
IHC	immunohistochemistry
ISH	in situ hybridization
pDC	plasmacytoid dendritic cell

References

1. Rerks-Ngarm S, et al. Vaccination with ALVAC and AIDSVAX to prevent HIV-1 infection in Thailand. N. Engl. J. Med. 2009; 361:2209–2220. [PubMed: 19843557]

2. Baeten J, Celum C. Systemic and topical drugs for the prevention of HIV infection: antiretroviral pre-exposure prophylaxis. Annu. Rev. Med. 2013; 64:219–232. [PubMed: 23020883]

3. Abdool Karim Q, et al. Effectiveness and safety of tenofovir gel, an antiretroviral microbicide, for the prevention of HIV infection in women. Science. 2010; 329:1168–1174. [PubMed: 20643915]

4. Grant RM, et al. Preexposure chemoprophylaxis for HIV prevention in men who have sex with men. N. Engl. J. Med. 2010; 363:2587–2599. [PubMed: 21091279]

5. Thigpen MC, et al. Antiretroviral preexposure prophylaxis for heterosexual HIV transmission in Botswana. N. Engl. J. Med. 2012; 367:423–434. [PubMed: 22784038]

6. Baeten JM, et al. Antiretroviral prophylaxis for HIV prevention in heterosexual men and women. N. Engl. J. Med. 2012; 367:399–410. [PubMed: 22784037]

7. Cohen MS, et al. Prevention of HIV-1 infection with early antiretroviral therapy. N. Engl. J. Med. 2011; 365:493–505. [PubMed: 21767103]

8. Tobian AA, Kacker S, Quinn TC. Male circumcision: a globally relevant but under-utilized method for the prevention of HIV and other sexually transmitted infections. Annu. Rev. Med. 2014; 65:293–306. [PubMed: 24111891]

9. Auvert B, Taljaard D, Lagarde E, Sobngwi-Tambekou J, Sitta R, Puren A. Randomized, controlled intervention trial of male circumcision for reduction of HIV infection risk: the ANRS 1265 Trial. PLoS Med. 2005; 2:e298. [PubMed: 16231970]

10. Bailey RC, et al. Male circumcision for HIV prevention in young men in Kisumu, Kenya: a randomised controlled trial. Lancet. 2007; 369:643–656. [PubMed: 17321310]

11. Gray RH, et al. Male circumcision for HIV prevention in men in Rakai, Uganda: a randomised trial. Lancet. 2007; 369:657–666. [PubMed: 17321311]

12. UNAIDS. Report on the global AIDS epidemic. 2013 http://www.unaids.org/sites/default/files/media_asset/UNAIDS_Global_Report_2013_en_1.pdf.

13. Haase AT. Targeting early infection to prevent HIV-1 mucosal transmission. Nature. 2010; 464:217–223. [PubMed: 20220840]

14. Miller CJ, et al. Propagation and dissemination of infection after vaginal transmission of simian immunodeficiency virus. J. Virol. 2005; 79:9217–9227. [PubMed: 15994816]

15. McMichael AJ, Borrow P, Tomaras GD, Goonetilleke N, Haynes BF. The immune response during acute HIV-1 infection: clues for vaccine development. Nat. Rev. Immunol. 2010; 10:11–23. [PubMed: 20010788]

16. Haase AT. Early events in sexual transmission of HIV and SIV and opportunities for interventions. Annu. Rev. Med. 2011; 62:127–139. [PubMed: 21054171]

17. Li Q, et al. Glycerol monolaurate prevents mucosal SIV transmission. Nature. 2009; 458:1034–1038. [PubMed: 19262509]

18. Shang L, et al. NK cell responses to simian immunodeficiency virus vaginal exposure in naive and vaccinated rhesus macaques. J. Immunol. 2014; 193:277–284. [PubMed: 24899503]

19. Smith AJ, et al. Live simian immunodeficiency virus vaccine correlate of protection: immune complex-inhibitory fc receptor interactions that reduce target cell availability. J. Immunol. 2014; 193:3126–3133. [PubMed: 25143442]

20. Zhang Z, et al. Sexual transmission and propagation of SIV and HIV in resting and activated CD4$^+$ T cells. Science. 1999; 286:1353–1357. [PubMed: 10558989]

21. Ma Z, Lu X, Torten M, Miller CJ. The number and distribution of immune cells in the cervicovaginal mucosa remain constant throughout the menstrual cycle of rhesus macaques. J. Immunol. 2001; 100:240–249.

22. Johnson RP, et al. Highly attenuated vaccine strains of simian immunodeficiency virus protect against vaginal challenge: inverse relationship of degree of protection with level of attenuation. J. Virol. 1999; 73:4952–4961. [PubMed: 10233957]

23. Johnson RP. Live attenuated AIDS vaccines: hazards and hopes. Nat. Med. 1999; 5:154–155. [PubMed: 9930861]

24. Wyand MS, Manson K, Montefiori DC, Lifson JD, Johnson RP, Desrosiers RC. Protection by live, attenuated simian immunodeficiency virus against heterologous challenge. J. Virol. 1999; 73:8356–8363. [PubMed: 10482586]

25. Li Q, et al. Live simian immunodeficiency virus vaccine correlate of protection: local antibody production and concentration on the path of virus entry. J. Immunol. 2014; 193:3113–3125. [PubMed: 25135832]

26. Parrish NF, et al. Phenotypic properties of transmitted founder HIV-1. Proc. Natl. Acad. Sci. U.S.A. 2013; 110:6626–6633. [PubMed: 23542380]

27. Zhang ZQ, et al. Roles of substrate availability and infection of resting and activated CD4$^+$ T cells in transmission and acute simian immunodeficiency virus infection. Proc. Natl. Acad. Sci. U.S.A. 2004; 101:5640–5645. [PubMed: 15064398]

28. Hrecka K, et al. Vpx relieves inhibition of HIV-1 infection of macrophages mediated by the SAMHD1 protein. Nature. 2011; 474:658–661. [PubMed: 21720370]

29. Laguette N, et al. SAMHD1 is the dendritic- and myeloid-cell-specific HIV-1 restriction factor counteracted by Vpx. Nature. 2011; 474:654–657. [PubMed: 21613998]

30. Prakash M, Patterson S, Gotch F, Kapembwa MS. Recruitment of CD4 T lymphocytes and macrophages into the cervical epithelium of women after coitus. Am. J. Obstet. Gynecol. 2003; 188:376–381. [PubMed: 12592243]

31. Arnold KB, et al. Increased levels of inflammatory cytokines in the female reproductive tract are associated with altered expression of proteases, mucosal barrier proteins, and an influx of HIV-susceptible target cells. Mucosal Immunol. 2016; 9:194–205. [PubMed: 26104913]

32. Masson L, et al. Genital inflammation and the risk of HIV acquisition in women. Clin. Infect. Dis. 2015; 61:260–269. [PubMed: 25900168]

33. Yao XD, et al. Acting locally: innate mucosal immunity in resistance to HIV-1 infection in Kenyan commercial sex workers. Mucosal Immunol. 2014; 7:268–279. [PubMed: 23801306]

34. Smith AJ, Li Q, Wietgrefe SW, Schacker TW, Reilly CS, Haase AT. Host genes associated with HIV-1 replication in lymphatic tissue. J. Immunol. 2010; 185:5417–5424. [PubMed: 20935203]

35. Smith AJ, Schacker TW, Reilly CS, Haase AT. A role for syndecan-1 and claudin-2 in microbial translocation during HIV-1 infection. J. Acquir. Immune Defic. Syndr. 2010; 55:306–315. [PubMed: 20700059]

36. Bannert N, Schenten D, Craig S, Sodroski J. The level of CD4 expression limits infection of primary rhesus monkey macrophages by a T-tropic simian immunodeficiency virus and macrophagetropic human immunodeficiency viruses. J. Virol. 2000; 74:10984–10993. [PubMed: 11069993]

37. Li Q, et al. Visualizing antigen-specific and infected cells in situ predicts outcomes in early viral infection. Science. 2009; 323:1726–1729. [PubMed: 19325114]

38. Pudney J, Quayle AJ, Anderson DJ. Immunological microenvironments in the human vagina and cervix: mediators of cellular immunity are concentrated in the cervical transformation zone. Biol. Reproduct. 2005; 73:1253–1263.
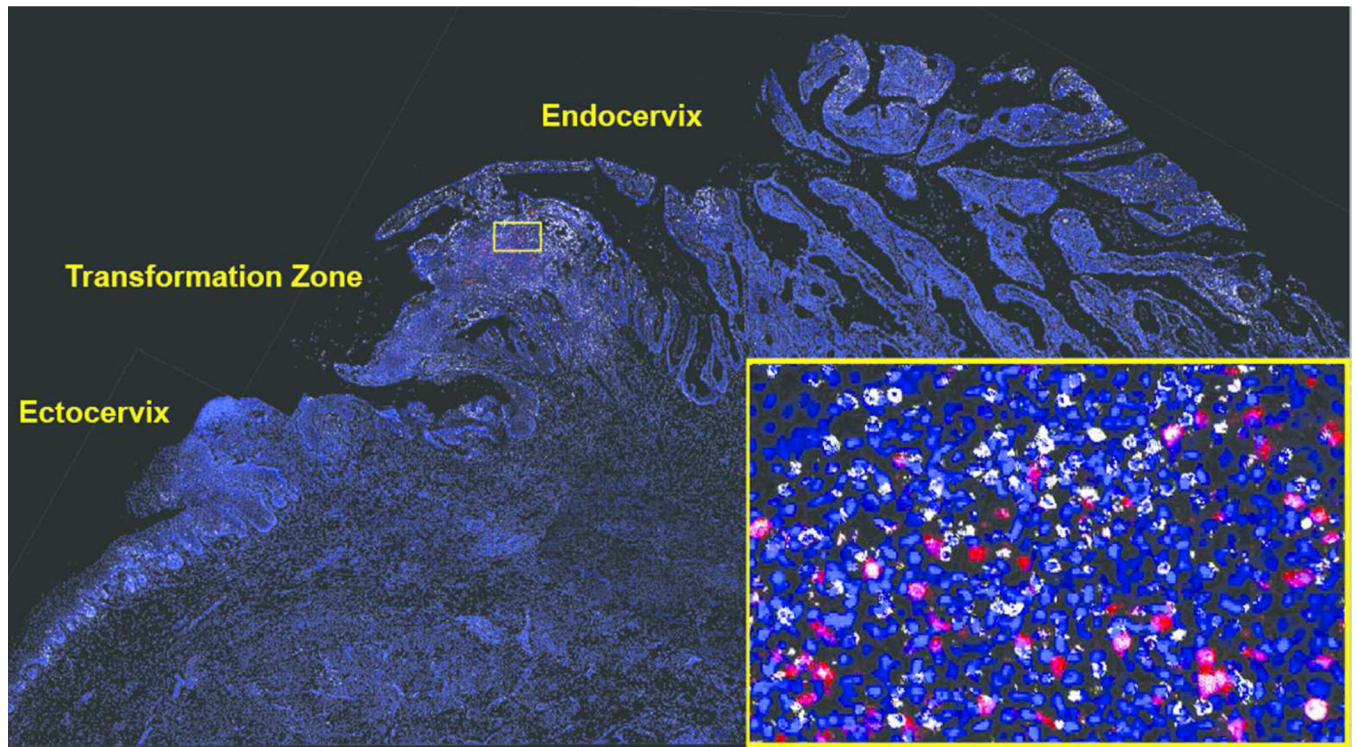
FIGURE 1.
Co-clustering of CD4 T cells (white) and SIV vRNA^{+} infected cells (red) in cervical mucosa close to the endocervical epithelium after vaginal challenge. The montage was constructed with images (original magnification ×200) of the cervical tissue from a rhesus macaque 7 days after vaginal infection with SIVmac251. Insert shows co-clustering in the marked region at higher magnification. The vRNA+ cells are predominantly CD4+ T cells (co-localized red and white).
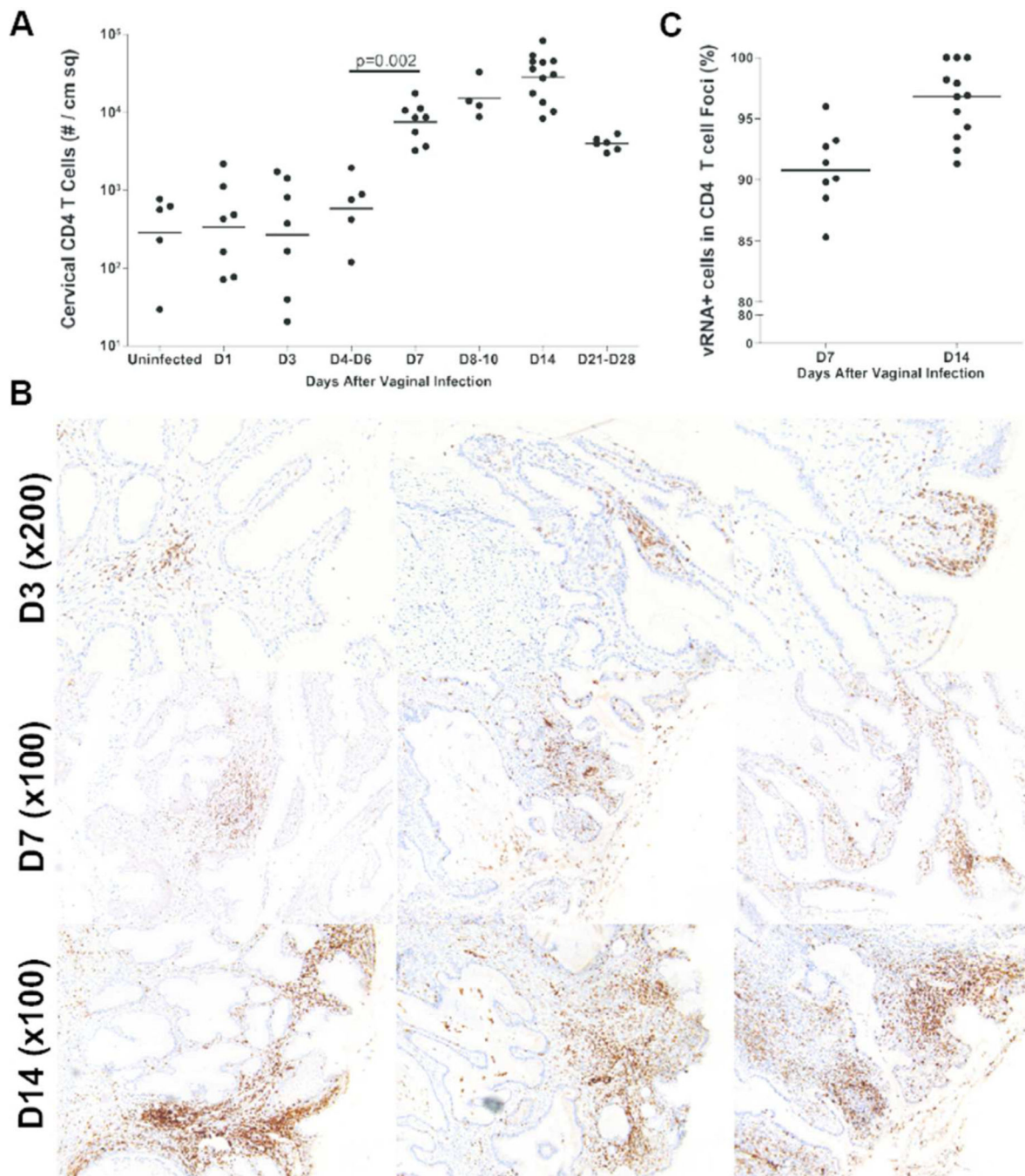
FIGURE 2.
Kinetics of accumulation of CD4+ T cells and vRNA+ cells beneath the epithelium of cervical transformation zone and adjoining endocervix. (A) Cervical CD4 T cells remained at basal levels at 3 d.p.i. but their numbers were significantly increased by 7 d.p.i. and peaked approximately at 14 d.p.i. before declining to levels still considerably higher than baseline levels by 28 d.p.i. (B) Representative images from 3 different animals for each time point in the kinetics of recruitment of brown-stained CD4 T cells beneath the endocervical epithelium. Clusters were first observed in some animals as early as at 3 d.p.i. (diameter

150±28 μm, CD4 T cells per cluster 36±12, n=15). By 7 d.p.i., clusters were detected in all examined animals, and by 14 d.p.i. the sizes of clusters and densities of CD4 T cells in the clusters increased dramatically. C) Local expansion in vRNA+ cells predominantly maps to CD4 T cell foci. Based on the sizes of CD4 T cells clusters at 3 d.p.i. and their cell densities, we defined in this study the minimal cluster as at least 24 CD4 T cells (the minimal number of CD4 T cells in clusters at 3 d.p.i.) within a range of 178μm in diameter (the maximal diameter of clusters at 3 d.p.i.). With this definition, we quantified the percentage of vRNA+ cells that fell into a minimal CD4 T cell cluster.
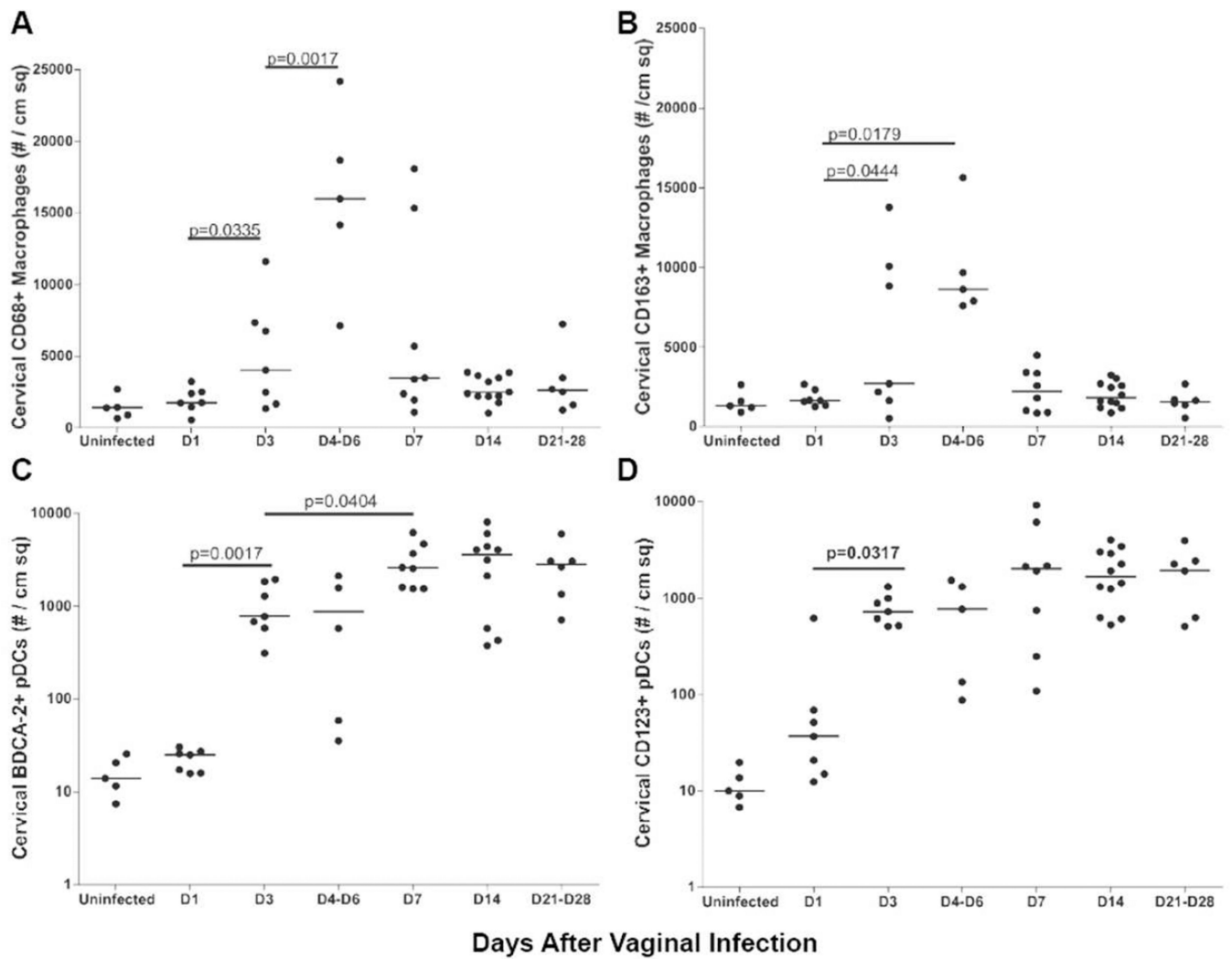
FIGURE 3.
The kinetics of accumulation of CD68^{+} (A) and CD163^{+} (B) macrophages and BDCA2^{+} (C) and CD123^{+} (D) pDCs in the cervical tissues over the course of vaginal infection. Macrophages and pDCs were temporally antecedent to CD4 T cell recruitment. Every dot represents an individual animal. At least 2–3 random cervical sections were stained and counted for every animal.
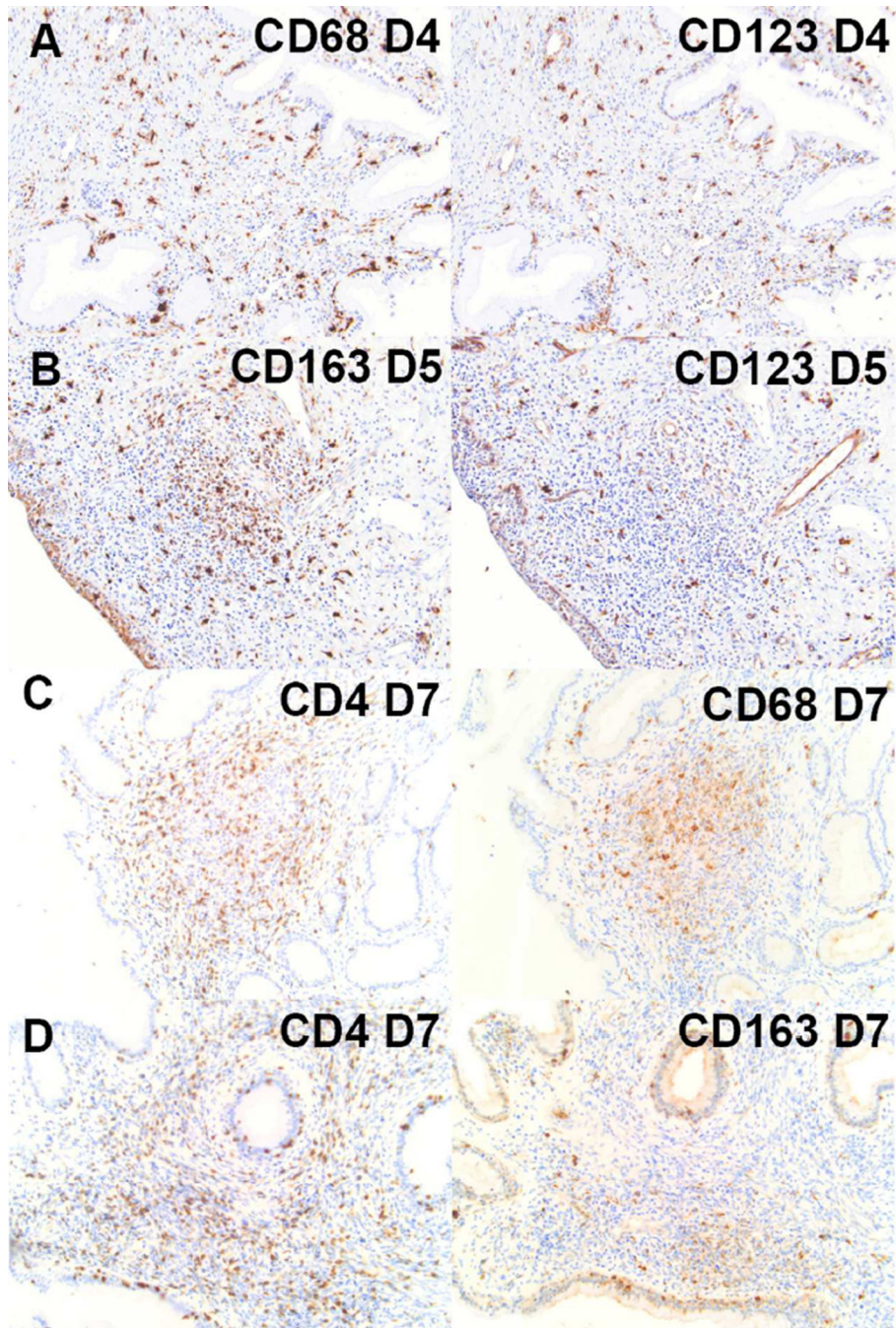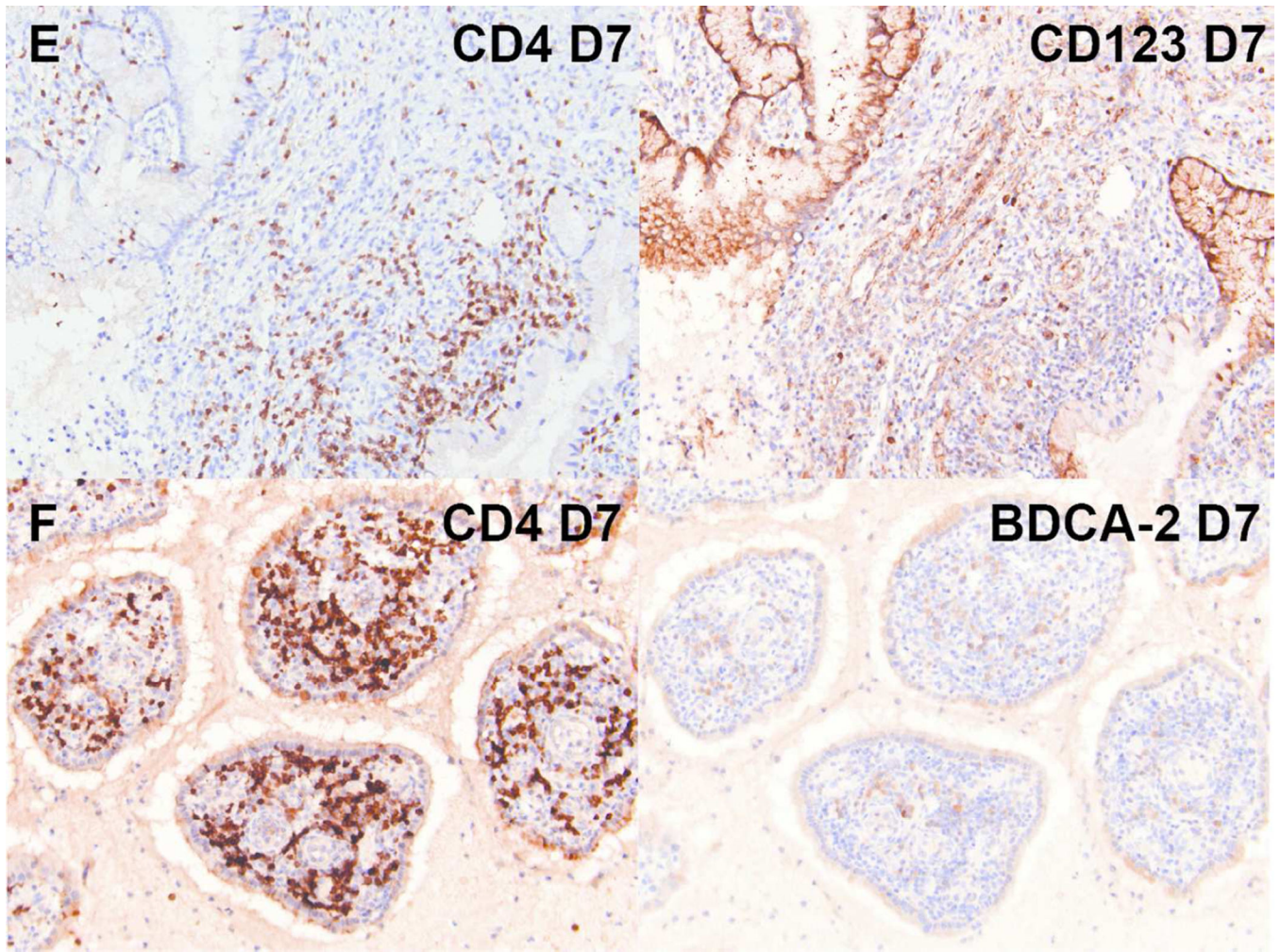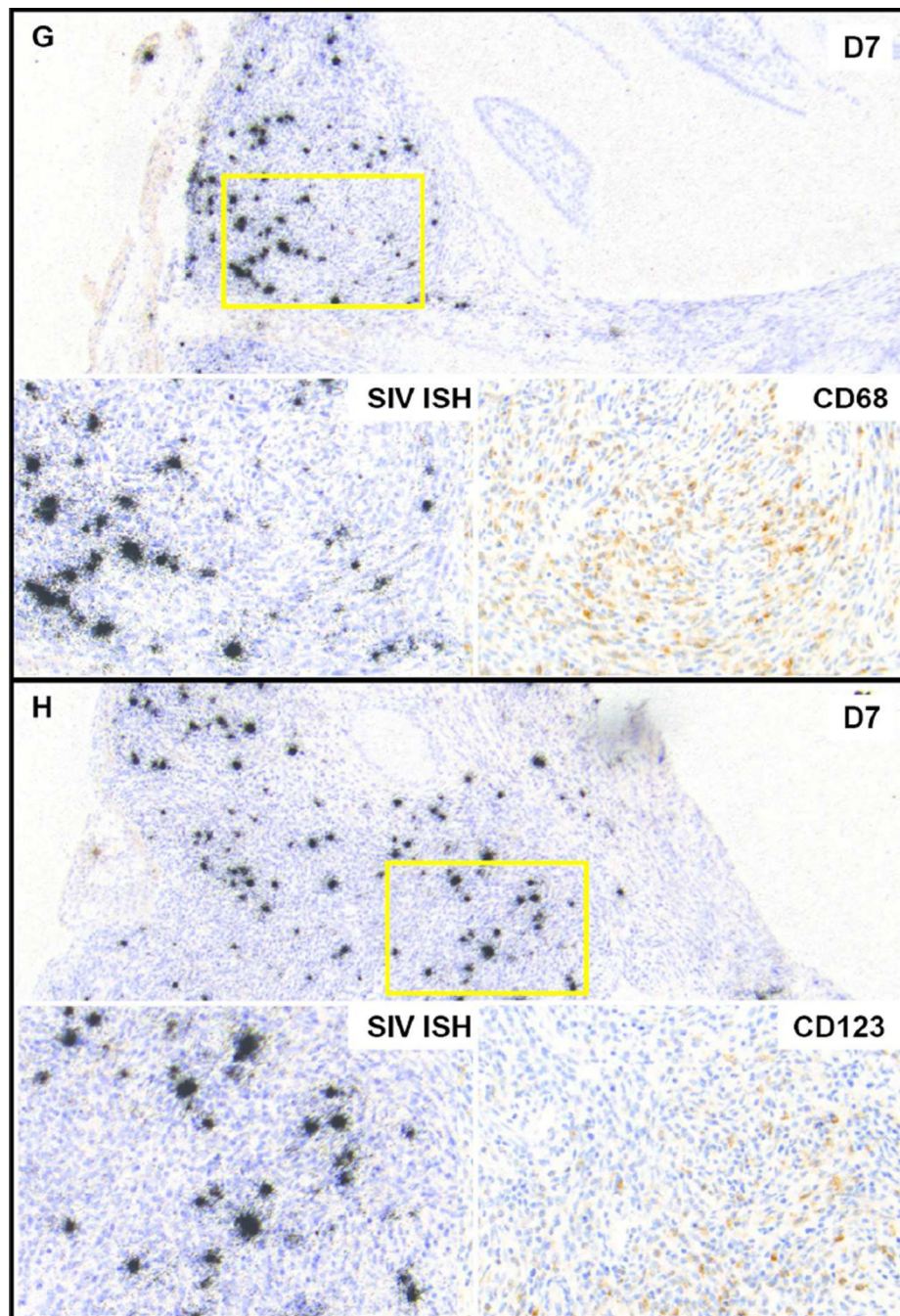
FIGURE 4.

Co-localization in subjacent tissue sections of CD4+ T cells, macrophages, pDCs and vRNA + cells (original magnification ×200) in the cervical transformation zone and adjoining endocervical tissues. Macrophages were defined as CD68+ and CD163+ cells; and pDCs as CD123+ and BDCA-2+ cells. (A–B) Macrophages and pDCs often co-cluster under the cervical epithelium, even prior to CD4 T cell recruitment. Representative images in each panel were obtained from 2 different animals (4–5 d.p.i.), in which CD4 recruitment was not yet detectable in the cervical tissues. (C–F) By 7 d.p.i., macrophages and pDCs were

consistently found to co-localize in cervical CD4 T cell foci in all 8 examined animals. Representative images in every panel were obtained from 4 different animals. Adjacent sections were used in panels A–F. (G–H) vRNA+ cells (appear black in transmitted light) were primarily localized in regions with macrophages and pDCs. Representative images in each panel were obtained from 2 different animals (7 d.p.i.).
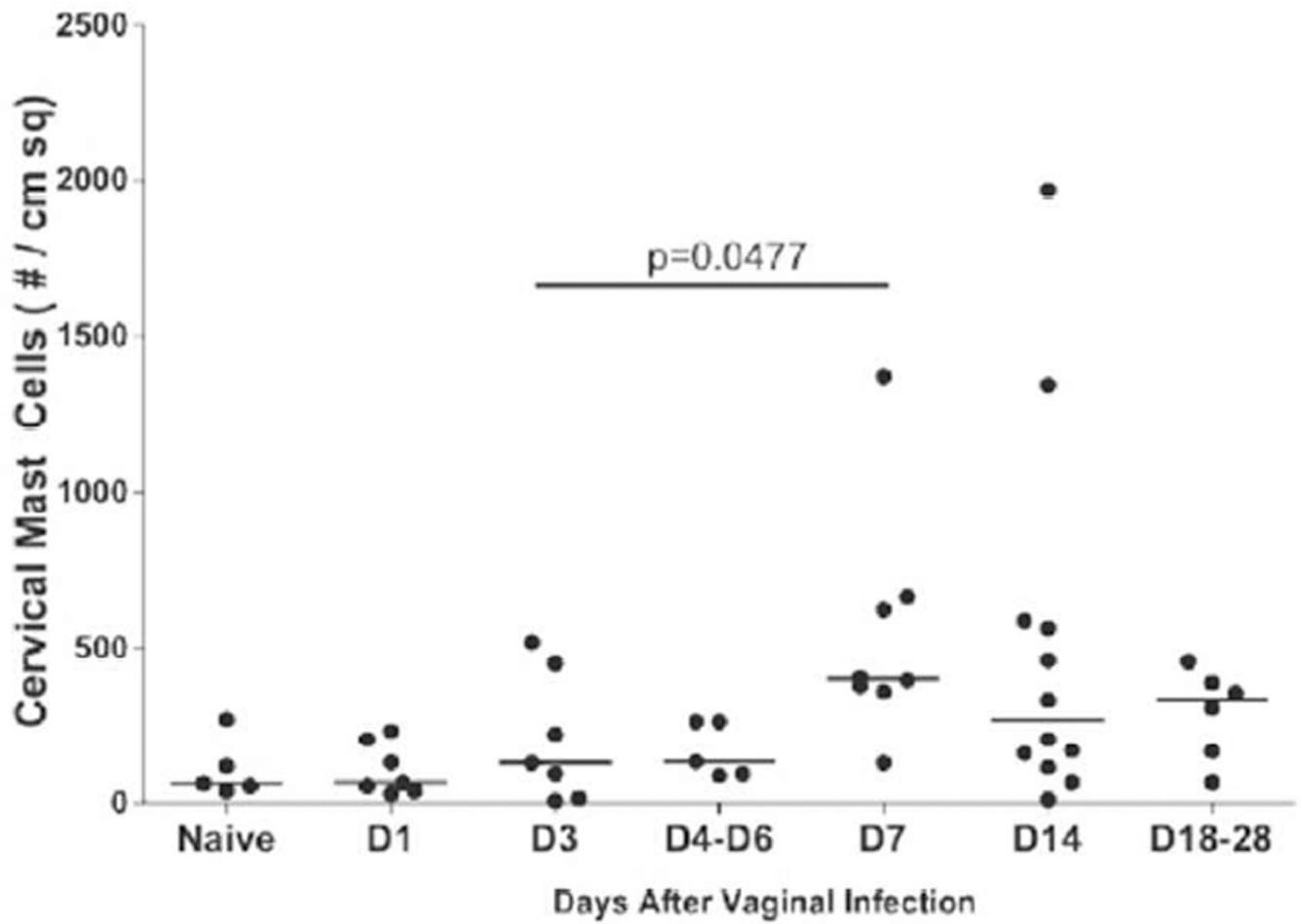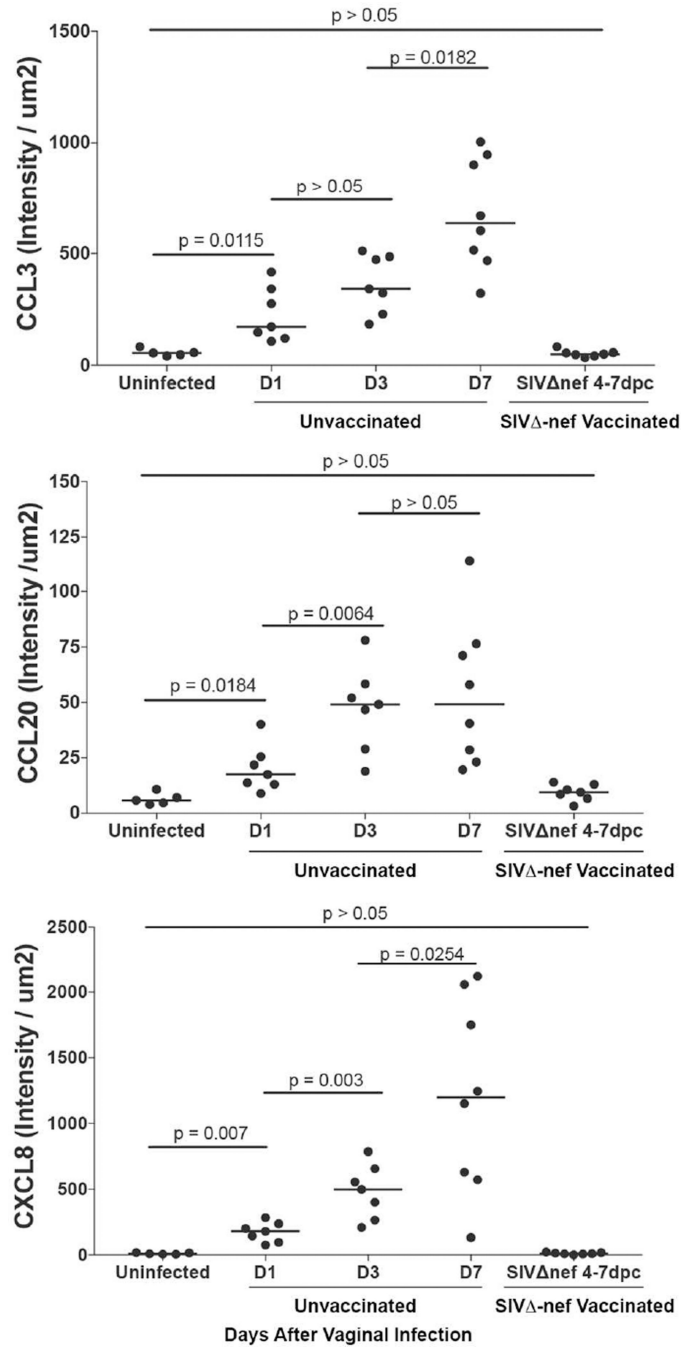
FIGURE 5.
The kinetics of mast cell accumulation in the cervical tissues. There was a slight increase in mast cells in the cervical tissues at 7 d.p.i.
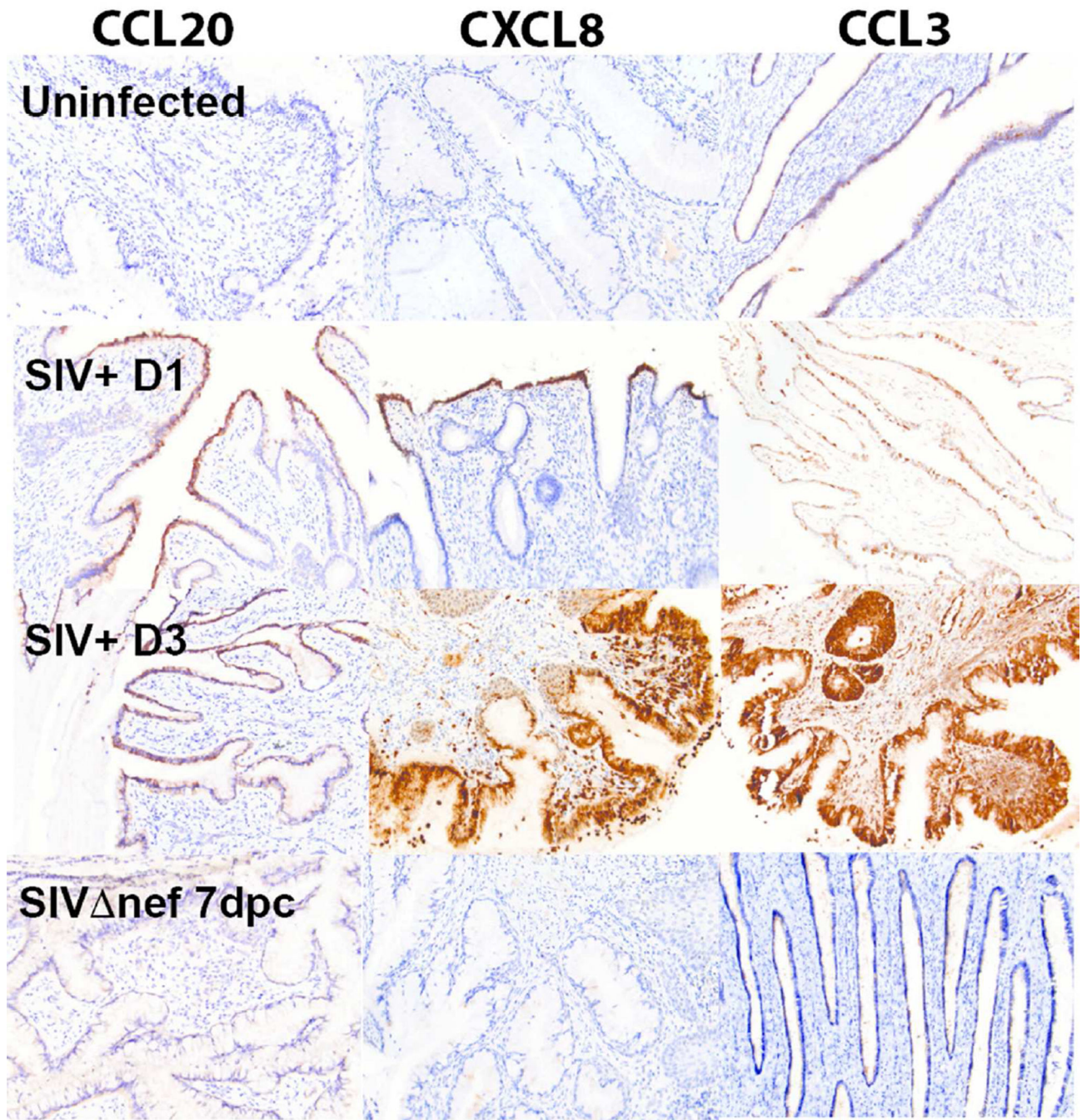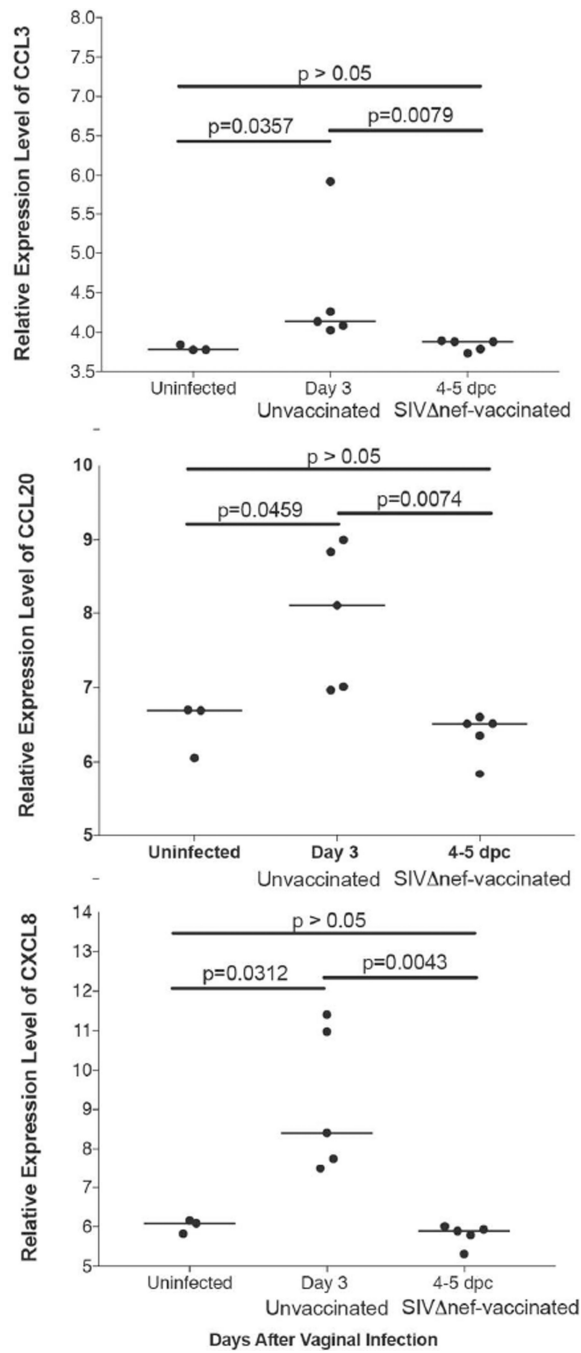
FIGURE 6.

Early chemokine expression in cervical tissues after vaginal challenge. (A) CCL20, CXCL8, and CCL3 were induced in the endocervical epithelium within 24h after vaginal inoculation. Epithelial expression of these chemokines persisted through the course of infection examined in this study. By contrast, these chemokine ligands were not expressed in the cervical tissues of SIVmac239 nef-vaccinated animals after SIV vaginal challenge. (Original magnification ×200) (B) Microarray analysis of cervical necropsy tissues showed that the transcriptional levels of CCL3, CCL20 and CXCL8 increased after vaginal infection
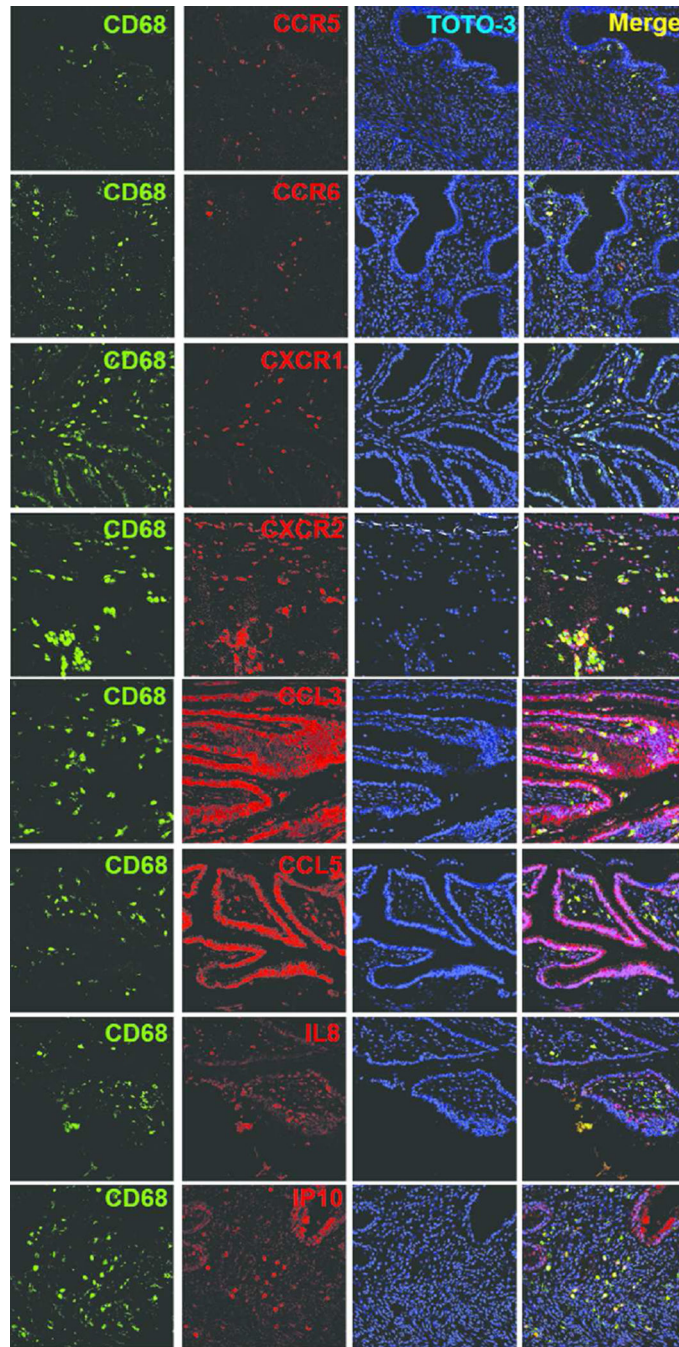
in unvaccinated animals, but remained at basal levels in SIVmac239 nef-vaccinated animals. (C) Quantitative image analysis (QIA): The expression of chemokines was quantified by measuring the intensities of pixel per μm^2 on IHC stained sections.
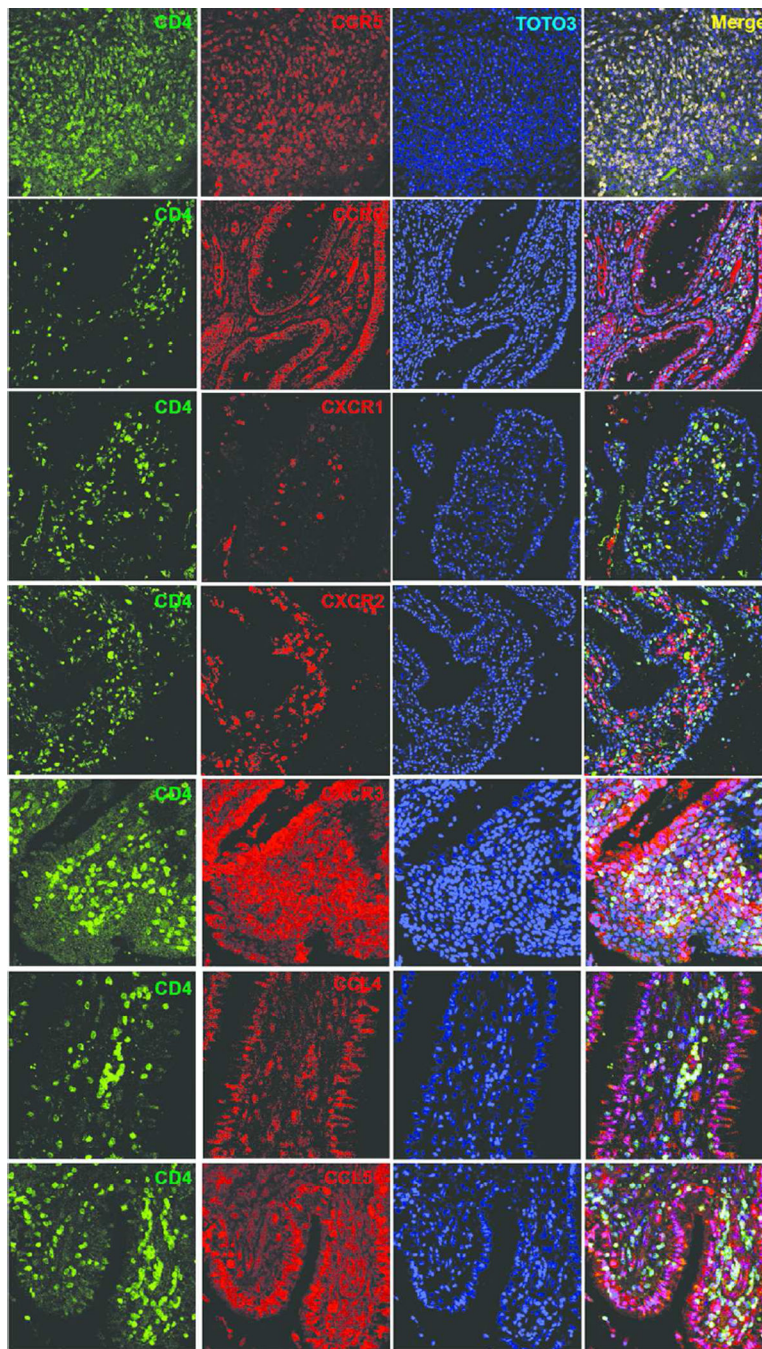
FIGURE 7.
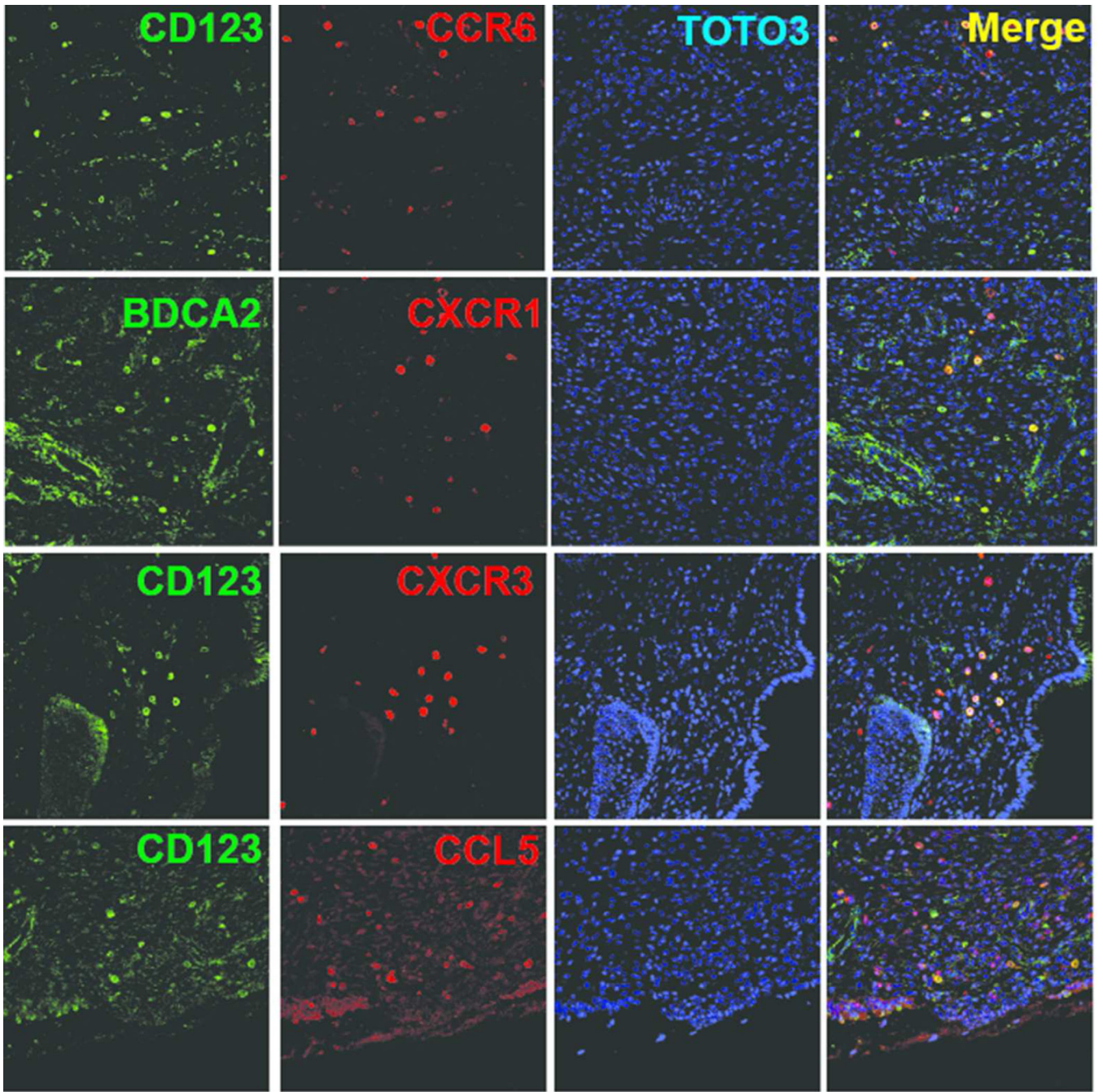Profiles of chemokine ligands and receptors induced in cervical macrophages (A), pDCs (B), and CD4 T cells (C) relevant to the recruitment by epithelial expression of CCL20, CCL3, and CXCL8, the co-clustering, and the chemokine concentration gradient. (A) Cervical macrophages (CD68^{+}) were CCR5^{+}, CCR6^{+}, CXCR1^{+}, and CXCR2^{+} and hence could be recruited by their ligands expressed in epithelium. Cervical macrophages produced CCL3, CCL5, CXCL8 (IL-8), and CXCL10/IP-10, the latter consistent with recruitment of CXCR3^{+} pDCs and CD4 T cells (B) Cervical pDCs (BDCA2^{+} or CD123^{+}) were CCR6^{+},

CXCR1^{+}, and CXCR3^{+}; hence could be recruited by ligands expressed in epithelium and macrophages. The recruited pDCs produced CCL5 as well. (C) Cervical CD4 T cells were CCR6^{+}, CXCR1^{+}, CXCR2^{+} and CXC3R^{+}; and expressed CCL4 and CCL5. The endocervical epithelium was also CXCL10 (A) and CCL4 positive (C) in some animals as shown in the figures, but we did not observe consistent expression of these chemokines in all examined animals. These montages were constructed with images with original magnification of ×200. Macrophages were profiled in cervical transformation zone and adjoining endocervical tissues from all animals at 3 d.p.i., pDCs at 3 d.p.i., and CD4 T cells at 7 d.p.i. Only the most representative images were shown here. Nuclei stained blue with TOTO-3. White dashed line marks the endocervical epithelium.
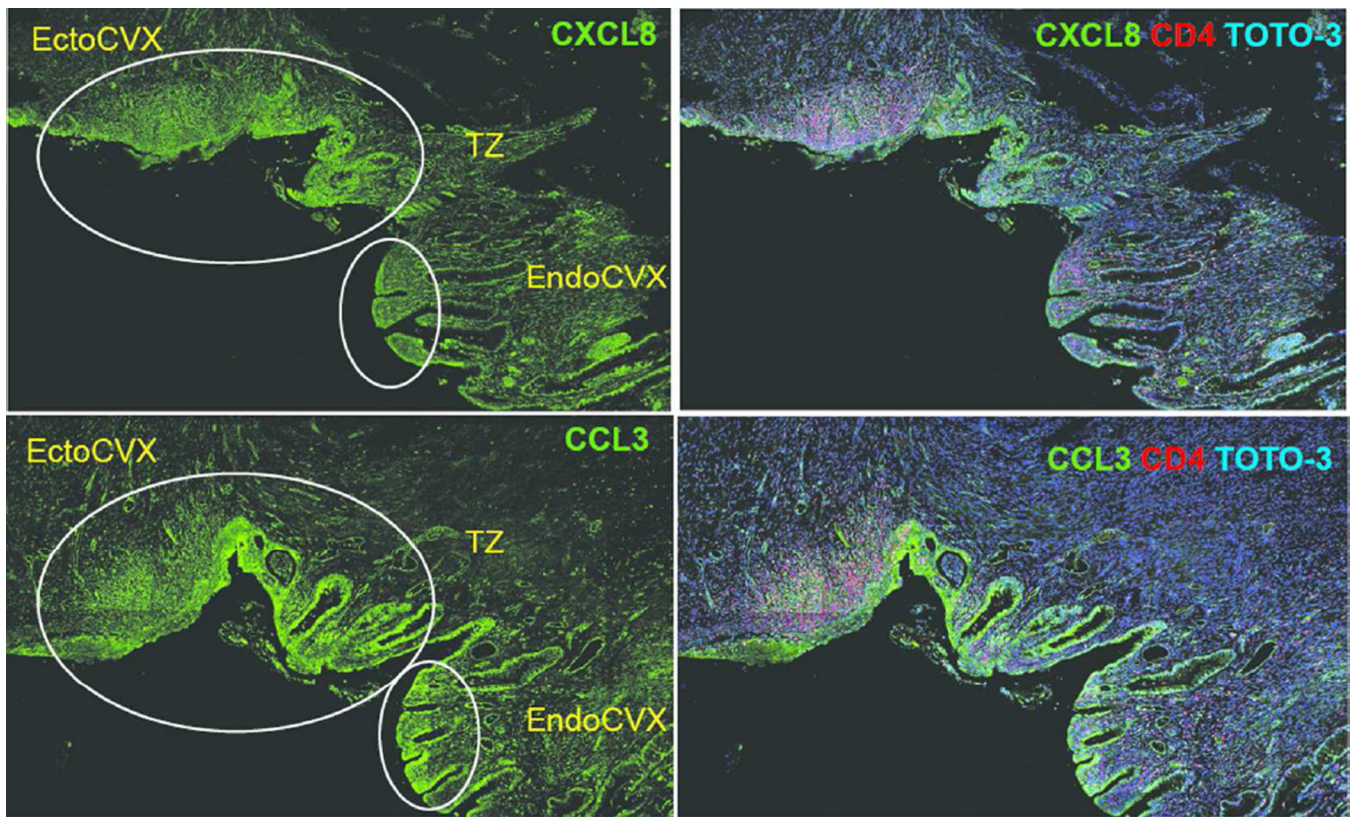
FIGURE 8.
Clustering of the recruited cells in foci where chemokines CXCL8 and CCL3 are concentrated beneath the cervical epithelium close to the cervical transformation zone (left panels, encircled). Recruited CD4 T cells (red) predominantly co-localize to these foci of concentrated chemokines (right). The representative montages were obtained from cervical tissues from an animal at 7 d.p.i. These montages were constructed with images with original magnification of ×200. TZ: transformation zone; EctoCVX: ectocervix; EndoCVX: endocervix.
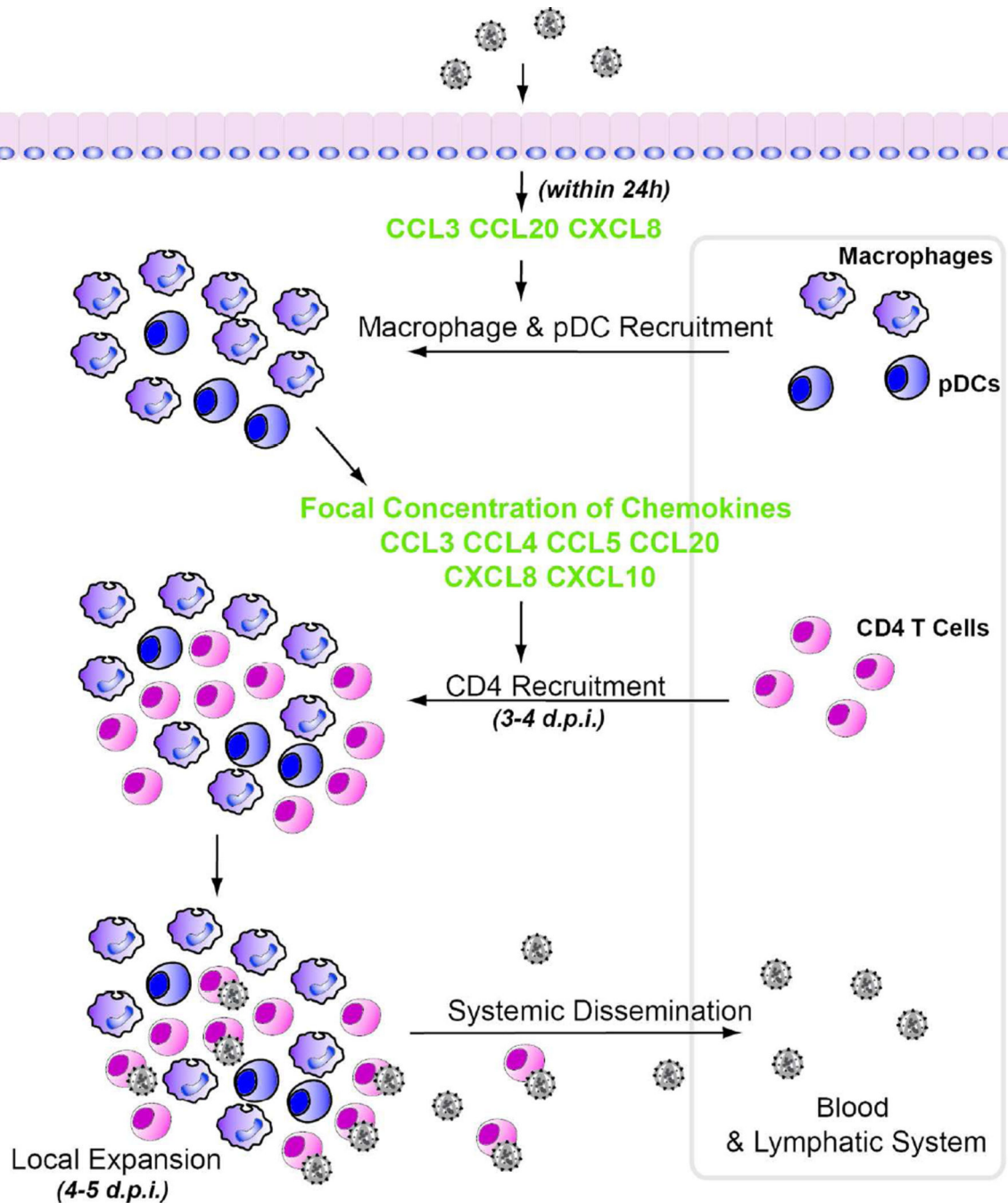
FIGURE 9.
Model of the epithelium-innate immune cell axis and the sequential events in early mucosal responses that lead to CD4$^+$ T cell recruitment. (1) Cervical epithelium responds to exposure to the SIV inoculum by producing CCL3, CCL20, and CXCL8; (2) the epithelial chemokines recruit macrophages and pDCs; (3) the macrophages and pDCs themselves produce CCL3, CCL5, CXCL8, and CXCL10 to create a focal concentrated source of chemokines beneath the epithelium; (4) this chemokine gradient recruits β-chemokine-

producing CD4 T cells along with more macrophages and pDCs to generate a positive feed forward mechanism to sustain further increases in CD4 T cell targets.

Table 1

Profiles of other cell types of leukocytes in the cervical transition zone after vaginal infection of SIV

Cell Types	Markers	Abundance	Co-cluster with CD4 T cells and vRNA+ cells
Eosinophil	BMK13	Not detected	-
Basophil	2D7	Not detected	-
Plasma Cell	CD138	Not detected	-
Myeloid Dendritic Cell (mDC) *	DC-SIGN S100B Fascin CD83	Not detected	-
Langerhans Cell *	CD1a Langerin	Not detected	No
B Cell	CD20	Not consistently detected	No
CD8+ Cell *	CD8	Not consistently detected	No
Neutrophil	Neutrophil Elastase Nuclei Morphology	Not consistently detected	No
NK Cell *	NKG2A	Small increase	No
Mast Cell	Mast Cell Tryptase Toluidine Staining	See Fig. 5	No

*: Consistent with previous reports.[18,27,37,38]

Table 2

Primary Abs used in this study[*]

Antigens	Clones & Producers	Fixation	Antigen Retrieval Conditions
CD4[**]	1F6 Vector (VP-C318)	PFA	1mM EDTA buffer pH8 98°C 20min
CD8α	1A5 Vector (VP-C325)	PFA	10mM citrate buffer pH6 98°C 20min
CD68	KP1 DAKO M0814	PFA	10mM citrate buffer pH6 98°C 20min
CD163	Vector VP-C374	PFA	10mM citrate buffer pH6 98°C 20min
BDCA-2	104C12.08 Dendritics DDX0041	SAFEFIX II	1mM EDTA buffer pH8 98°C 20min
CD123	V-18 Santa Cruz sc-681	PFA	10mM citrate buffer pH6 98°C 20min
c-Kit	Novus Biologicals NBP1-85593	SAFEFIX II	10mM citrate buffer pH6 98°C 20min
CCL3	Neomarkers RB-10489-P	PFA	10mM citrate buffer pH6 98°C 20min
CCL4	R&D AF-271-NA	PFA	10mM citrate buffer pH6 98°C 20min
CCL5	R&D AF-278-NA	PFA	10mM citrate buffer pH6 98°C 20min
CCL20	2069D.05 / Dendritics & # DDX0420	PFA	1mM EDTA buffer pH8 98°C 20min
IL-8	Abcam ab7747-500	PFA	10mM citrate buffer pH6 98°C 20min
IP10	R&D AF-266-NA	PFA	10mM citrate buffer pH6 98°C 20min
CCR5	AIDS Reagents 4914	PFA	1mM EDTA buffer pH8 98°C 20min
CCR6	R&D MAB195	PFA	10mM citrate buffer pH6 98°C 20min
CXCR1	Novus Biologicals NBP1-88143	SAFEFIX II	1mM EDTA buffer pH8 98°C 20min
CXCR2	Novus Biologicals NBP1-02412	PFA	10mM citrate buffer pH6 98°C 20min
CXCR3	R&D 49801 MAB160	PFA	10mM citrate buffer pH6 98°C 20min
BMK13	Abcam 77842	PFA	10mM citrate buffer pH6 98°C 20min
CD138	AnaSpec 53317	PFA	10mM citrate buffer pH6 98°C 20min
DC-SIGN	R&D MAB161	PFA	10mM citrate buffer pH6 98°C 20min
S100B	Thermo Scientific MA5-15359	PFA	10mM citrate buffer pH6 98°C 20min
Fascin	Vector Lab VP-F703	PFA	10mM citrate buffer pH6 98°C 20min
CD83	Vector Lab VP-C368	PFA	10mM citrate buffer pH6 98°C 20min
CD1a	DAKO 3571	PFA	10mM citrate buffer pH6 98°C 20min
Langerin	Vector Lab VP-L552	PFA	10mM citrate buffer pH6 98°C 20min
Elastase	DAKO 0752	PFA	10mM citrate buffer pH6 98°C 20min
NKG2A	Epitomics T3308	PFA	10mM citrate buffer pH6 98°C 20min
Tryptase	DAKO M7052	PFA	10mM citrate buffer pH6 98°C 20min

Notes:

[*] Isotype controls were performed on all examined animals (See Supplementary Fig. 1).

[**] CD4 Ab concenration was optimized to only stain CD4+ T cells that have higher CD4 expression than macrophages[36] (See Supplementary Fig. 2).